J Membrane Biol (2009) 230:69–81
DOI 10.1007/s00232-009-9187-z

Formation of Two Different Types of Ion Channels by Amphotericin B in Human Erythrocyte Membranes

Eneida A. Romero · Elizabeth Valdivieso · B. Eleazar Cohen

Received: 22 January 2009 / Accepted: 17 June 2009 / Published online: 23 July 2009

Abstract The polyene antibiotic amphotericin B (AmB) is known to form aqueous pores in lipid membranes and biological membranes. Here, membrane potential and ion permeability measurements were used to demonstrate that AmB can form two types of selective ion channels in human erythrocytes, differing in their interaction with cholesterol. We show that AmB induced a cation efflux (negative membrane polarization) across cholesterol-containing liposomes and erythrocytes at low concentrations ($\leq 1.0 \times 10^{-6}$ M), but a sharp reversal of such polarization was observed at concentrations greater than 1.0×10^{-6} M AmB, an indication that aqueous pores are formed. Cation-selective AmB channels are also formed across sterol-free liposomes, but aqueous pores are only formed at AmB concentrations 10 times greater. The effect of temperature on the AmB-mediated K^+ efflux across erythrocytes revealed that the energies of activation for channel formation are negative and positive at AmB concentrations that lead predominantly to the formation of cation-selective channels and aqueous pores, respectively. These findings support the conclusion that the two types of AmB channels formed in human erythrocytes differ in their interactions with cholesterol and other membrane components. In effect, a membrane lipid reorganization, as induced by incubation of erythrocytes with tetrathionate, a cross-linking agent of the lipid raft–associated protein spectrin, led to differential changes in the activation parameters for the formation of both types of channels, reflecting the different lipid environments in which such structures are formed.

Keywords Amphotericin B · Erythrocyte · Ion channel · Cholesterol · Lipid raft · Activation energy · Membrane potential

E. A. Romero · E. Valdivieso
Institute of Experimental Biology, Faculty of Sciences, Central University of Venezuela, Caracas, Venezuela

B. E. Cohen (✉)
Division of External Activities, National Institute of Allergy and Infectious Diseases, 6700B Rockledge Drive, Bethesda, MD 20982, USA
e-mail: ec17w@nih.gov

Introduction

For more than 50 years, the polyene antibiotic amphotericin B (AmB) mixed with deoxycholate in the conventional commercial preparation of Fungizone® (Bristol-Myers Squibb, Princeton, NJ) has been the "gold standard" for the treatment of life-threatening systemic fungal infections and visceral leishmaniasis in spite of toxic side effects (Gallis et al. 1990; Sundar et al. 2007). During the 1970s, the development of thin lipid bilayers and liposomes as models of biological membranes played an important role in the recognition of the ability that AmB and nystatin, a closely related polyene antibiotic, have to form aqueous pores of about 0.4 nm in radius (Finkelstein and Holz 1973; Cohen 1975). The membrane formation by AmB and nystatin of the aqueous pores was envisaged to produce a drastic disruption of the normal cell membrane's permeability barrier, and as a consequence, the fungicidal as well as the toxic side effects in host cells ensued. In the original "aqueous pore" model proposal (De Kruijff and Demel 1974) or its refinements (Van Hoogevest and De Kruijff 1978), AmB selectivity toward biological membranes was thought to arise from the higher affinity of the antibiotic toward ergosterol, the principal fungal sterol, than to cholesterol, the mammalian sterol.

In the last few years, increasing evidence obtained by using lipid membrane models and biological membranes has indicated that AmB can form various types of ion channels, with or without the direct participation of the membrane sterol. In liposomes (Cohen 1992) and membranes of ergosterol-containing sensitive organisms (Ramos et al. 1996), it was demonstrated that AmB can form at least two types of membrane channels, nonaqueous channels and aqueous pores, differing in their cation/anion selectivity. A two-stage mechanism for the interaction of ergosterol-containing membranes with the closely related polyene antibiotic nystatin has also been recently proposed (Coutinho et al. 2004). These authors have found that, at low concentrations, nystatin molecules can interact with liposome membranes, leading to a partial K^+ leakage, but it is only above a critical "threshold" concentration (about 100 membrane-bound antibiotic molecules per liposome) that the rate of channel formation sharply increased, leading to complete dissipation of the K^+ gradient across the membrane. The measurements of the nystatin-induced permeabilization of liposomes prepared with a mixture of ergosterol and cholesterol were also found to be biphasic and dependent on the ergosterol/cholesterol molar ratio, supporting the view that, above the critical "threshold" concentration, both sterols compete for the binding of nystatin, previous to the formation of the ion channels (Silva et al. 2006).

The formation of more than one type of ion channel by AmB is also strongly supported by studies in lipid bilayers, prepared from lipids with or without sterols, that have indicated the formation by AmB molecules of single channels exhibiting different conductances and probabilities of appearance (Venegas et al. 2003). However, the single-channel conductivities of the different AmB ion channels recorded by these investigators in lipid bilayers were found to be independent of the presence of either ergosterol or cholesterol in the membrane. In this respect, the lack of conclusive evidence for the existence of direct AmB–cholesterol interactions in the formation of some types of AmB channels may reflect differences in the lipid environment in which such structures are formed in model membrane systems compared to biological membranes. The formation of AmB/cholesterol complexes may depend on specific membrane factors, e.g., differences of the lateral distribution of cholesterol and lipid composition among certain regions of the biological membranes, that would facilitate the insertion of AmB molecules in ordered saturated membrane domains (Czub and Baginski 2006) such as the cholesterol-containing lipid rafts (Barenholz 2002; Simons and Vaz 2004). Indeed, the higher affinity that the AmB molecules are known to have for liquid-ordered l_o membrane domains of dimiristoyl-phosphatidylcholine (DMPC) liposomes determines that AmB can form the ion channels at lower concentrations in saturated membranes compared to membrane domains rich in unsaturated lipid hydrocarbon chains (Cohen 1992).

In erythrocyte membranes, lipid rafts that are isolated as the so-called detergent-resistant membranes (DRMs) are enriched with cholesterol and saturated molecular species of sphingomyelin in a molar ratio close to 1 (Koumanov et al. 2005). In the formation of the lipid rafts, lipid–lipid interactions are known to play an important role, i.e., cholesterol–sphingomyelin interactions (Ohvo-Rekila et al. 2002) as well as the interactions of such microdomains with proteins of the cytoskeleton (Salzer and Prohaska 2001; Ciana et al. 2005). Of note, spectrin, one of the major protein components of the cytoskeleton, is known to interact strongly with phospholipids (Grzybeck et al. 2006); and this protein has been partly associated with the lipid rafts in nonerythroid cells (Nebl et al. 2002) and in erythrocytes (Salzer and Prohaska 2001; Ciana et al. 2005; Crepaldi Domingues et al. 2009).

In the present work, we measured the effect of increasing AmB concentrations on the membrane potential across liposomes prepared with and without cholesterol and human erythrocytes using the fluorescence changes of 3,3′-dipropylthiadicarbocyanine ($DiSC_3[5]$) (Hladky and Rink 1976). We used flame emission photometry to measure the AmB-induced changes on the erythrocyte intracellular ion concentrations to K^+, Na^+ and Ca^{2+} ions. Activation parameters were also determined for the AmB-mediated K^+ exchange and Ca^{2+} influx across erythrocyte membranes by performing permeability measurements at different temperatures. Finally, we determined how the activation parameters to K^+ efflux were affected by tetrathionate (TT), a sulfhydryl-oxidizing agent that produced a cross-linking of spectrin that appears to increase the exposure of cholesterol at the membrane external leaflet (Lange et al. 2007) by inducing loss of the characteristic phospholipid asymmetry of the erythrocyte membranes (Haest et al. 1978). The present findings are discussed in terms of the formation by AmB in human erythrocytes of two types of ion channels, differing in their interactions with the membrane components.

Materials and Methods

Materials

Fresh blood from healthy donors (mainly O^+ group) was used throughout the investigation. AmB was obtained from Sigma (St. Louis, MO). Sodium TT (Sigma), di-*n*-butylphthalate (British Drug House, Poole, UK) and all organic solvents were of analytical grade and used without further purification. Stock solutions of AmB were prepared with dimethylsulfoxide (DMSO) or dimethylformamide (DMF).

Concentrations of AmB were determined using extinction coefficients (e at 409 AmB–DMF 123,000 M^{-1} cm^{-1} and e at 416 AmB–DMSO 121,400 M^{-1} cm^{-1}, as previously described [Readio and Bittman 1972; Legrand et al. 1992]).

Preparation of Human Erythrocytes

Fresh human blood was centrifuged at 3,000×*g* for 10 min at room temperature. After removing white cells, the suspension was adjusted to pH 7.4 and erythrocytes were washed three or four times with a 150 mM NaCl, 10 mM Tris–HCl (pH 7.4) medium. Cells were finally packed at 3,000×*g* for 20 min. Packed cells were hemolyzed with distilled water 1:20 in duplicate. In control preparations, the resulting lysate was used for potassium, sodium and/or calcium concentration determinations in order to correct for extracellular space. To correct for volume changes incurred during incubation, cellular volume was quantified by the cyanomethemoglobin method using absorption determinations at 540 nm (Drabkin and Austin 1932).

AmB Incubation

Erythrocytes were incubated at a final 2% hematocrit, equivalent to 2×10^8 cells suspended in NaCl–sucrose (2:1) isotonic solution (NaCl 116 mM, sucrose 62 mM), adjusted with Tris–HCl buffer to pH 7.4. After temperature equilibration, AmB from a 1 mM stock in either DMSO or DMF was added at various concentrations and incubated for different times. The suspensions were immediately mixed by vortexing and light-protected. For kinetic measurements, samples were withdrawn at different time intervals, which were chosen depending on the concentration of AmB used. They were then rapidly squirted into ice-cooled Eppendorf tubes, to which 0.1 ml dibutylphthalate (DBP, density 1.042–1.043) was added, as described previously (Romero and Romero 1997). After 3-min centrifugation at 42,000×*g*, the supernatant was removed by aspiration, the walls of the tubes were cleaned with cotton swabs and the cells were finally lysed in water. The samples were again centrifuged at 42,000×*g* for 7 min to separate membrane residues and DBP and thereafter used for cation determinations by flame photometry and hemoglobin determinations. Potassium was determined by flame emission at 766.4 nm and sodium at 589 nm (Varian Techtron Model 1000 atomic absorption spectrophotometer; Varian, Inc., Palo Alto, CA), with appropriate dilutions in controls and samples, correcting for extracellular space ion content and expressing concentrations as microequivalents per milliliter of cells. Rate constants (*k*) for potassium efflux were calculated from the slope of regression curves relating cell potassium content to time and represent a measure of the permeabilizing action induced by AmB on human erythrocytes. Of note, the concentration of the stock solution of AmB (in DMSO or DMF) was always kept at 1 mM to control for the proportion of different forms of AmB present in water, which are known to affect the kinetics of K^+ release from erythrocytes (Legrand et al. 1992). Thus, as we have shown previously, the addition of different amounts of solvent did not change the kinetics of the measurements (Legrand et al. 1992).

Measurements of Membrane Potential Changes

AmB-induced membrane potential changes (ΔVm) across liposomes and erythrocyte membranes were followed by using the fluorescence changes of $DiSC_3(5)$ as previously described (Ramos et al. 1996); fluorescence measurements were carried out using a Fluorolog II spectrophotometer (SPEX, Edison, NJ) equipped with a magnetic stirrer at 620 and 670 nm excitation and emission wavelengths, respectively. Large unilamellar vesicles (LUVs) were formed by the reverse-phase evaporation method, as described previously (Cohen 1992). In a typical protocol, liposomes prepared containing egg-phosphatidylcholine (eggPC + 16 mol% cholesterol [or pure eggPC]) in a 100 mM KCl solution were added to a fluorescence cuvette containing 200 mM sucrose solution (final lipid concentration 0.05 mM). $DiSC_3(5)$ (stock 0.6 mM in ethanol) was then added at a final concentration of 2×10^{-6} M. The fluorescence of the positively charged $DiSC_3(5)$ is rapidly quenched whenever it concentrates into the liposomes by the formation of a negative diffusion potential inside. Thus, by adding valinomycin (2 μM), maximum quenching was always obtained as a result of the movement of internal K^+ into the external sucrose medium driven by its concentration gradient.

For the corresponding membrane potential measurements across human erythrocyte membranes, cells (25×10^6/ml) were transferred to a fluorescence cuvette containing 2 ml of iso-osmotic sucrose buffer solution (pH 7.4). Gentle stirring ensured the homogeneity of the suspension during recordings. Upon addition of $DiSC_3(5)$ (3×10^{-6} M final concentration), the fluorescence signal slowly decreased, indicating uptake of the probe into the cells (time constant 3–5 min), driven by the existence of a negative membrane potential across human erythrocytes (Hladky and Rink 1976). All fluorescence measurements were carried out at room temperature.

Sodium Net Influx

Erythrocytes were incubated as described above with different AmB concentrations at 37°C for 30 min. To determine Na^+ and K^+ content by flame photometry, cells were separated from the medium with DBP, washed twice with

isotonic sucrose and lysed with 1 ml water. The error between replicate determinations was usually <5%.

Total Calcium Determinations

Calcium concentration was determined in cell lysates of control and incubated samples that were diluted by half in a medium that contained K^+ (5,000 μg/ml), lanthanum chloride (50 mM) and trichloroacetic acid (TCA) 5%. Protein sediments were eliminated after 42,000×*g* during 7 min centrifugation, and absorbance of the supernatant was determined at 422.5 nm by atomic absorption. Calcium concentrations were expressed as micromoles of Ca^{2+} per milliliter of cells.

Calcium Net Influx

ATP-depleted cells were prepared from fresh human erythrocytes by preincubation with 1 mM sodium iodoacetate, 160 mM NaCl, 5 mM KCl, 10 mM inosine and 20 mM Tris–HCl at a pH of 7.4 for 1 h at 37°C and 25% hematocrit (Romero and Romero 1997). In order to study the effect of AmB on calcium influx, incubation was performed at 10% hematocrit (2×10^7 cells) for 15 min at pH 7.4 in medium containing 110 mM KCl, 62 mM sucrose, 10 mM $CaCl_2$ and 20 mM Tris–HCl (336 mOsm) at pH 7.4 with different amounts of the polyene antibiotic. At each concentration, samples were incubated at 5 and 37°C and calcium influx was determined as $[Ca^{2+}]_f - [Ca^{2+}]_i$ (in micromoles calcium per milliliter cells).

Incubation Procedure with TT

Erythrocytes from freshly collected heparinized human blood were washed three times with an isotonic NaCl solution containing Tris–HCl 20 mM (pH 8). An aliquot of cells was taken for microscopic examination before incubation with TT. Erythrocytes (1 ml 10% hematocrit) were suspended in medium containing (mM) KCl 90, NaCl 25, sucrose 62, Tris–HCl 20 and sodium TT 2 mM and 20 mM at 37°C and pH 8.0 for 1 h, as previously described (Haest et al. 1978). Cells were centrifuged and washed once with the same medium. After that, they were incubated for 2 h at 37°C in the same medium (10% hematocrit) but without TT. In order to determine the cell K^+ content before and after incubation with the oxidizing agent, duplicate aliquots were taken and lysed with bidistilled water (1/20; v/v). After a further washing, they were suspended in NaCl–sucrose isotonic solution to study the effect of AmB on the K^+ permeability from these cells. Incubation of the erythrocytes with 20 mM TT produced a loss of about 20–30% of intracellular potassium, but due to the high content of potassium, K^+ permeability experiments could be performed at two AmB concentrations (2×10^{-6} and 10×10^{-6} M) at two temperatures (5 and 37°C). For this purpose, cells were further washed and suspended in NaCl–sucrose isotonic medium but without the oxidizing agent.

Gel Electrophoresis Analysis

Erythrocyte membranes were obtained following the method of Dodge et al. (1963). Briefly, packed cells (0.5 ml) previously incubated with or without TT were lysed (1/10, v/v) in a hypotonic solution containing (mM) NaCl 20 and Tris–HCl 10 (adjusted to pH 7.6) for 5 min at 0°C. Hemoglobin was removed by repeated washing with these solutions; the membranes were then kept at −70°C until further use. Gel electrophoresis was carried out essentially as described (Laemmli 1970). Incubation of erythrocytes with 2 and 20 mM TT concentrations led to a gradual disappearance of the spectrin bands that are observed by gel electrophoresis in control untreated samples (results not shown). As previously demonstrated, the disappearance of the bands is due to the formation of higher-molecular weight oligomers by the oxidative cross-linking of spectrin (Haest et al. 1978).

Results

Kinetics of K^+ Efflux from Human Erythrocytes at Increasing AmB Concentrations

The addition of AmB (dissolved in an appropriate organic solvent such as DMF) at increasing concentrations into an aqueous solution is known to lead to the formation of at least three distinct forms of AmB: monomeric, self-associated soluble dimers and insoluble oligomer aggregates (Legrand et al. 1992). If the monomeric forms of AmB dissolved in water are the active forms leading to channel formation after inserting into the membrane phase, it can be expected that the kinetics of the K^+ efflux from cells will vary linearly with the total external AmB concentrations. Figure 1 shows an example of a typical set of measurements of the kinetics of K^+ efflux from human erythrocytes (vs. time) at three different external AmB concentrations. The slope of these curves corresponds to the rate constant (k) for the K^+ efflux, according to a first-order rate process. The calculated k values for each of the AmB concentrations shown are plotted as a function of the AmB concentration (inset to Fig. 1). It can be seen that the dose–response curve (plotted in the inset using a log–log scale) is linear and that the slope is greater than 1. Such a linear plot indicates that the rate constants for K^+ efflux can be described by the equation $k = a\,[\mathrm{AmB}]^n$, where a is a constant, n is the cooperativity index and [AmB] is the

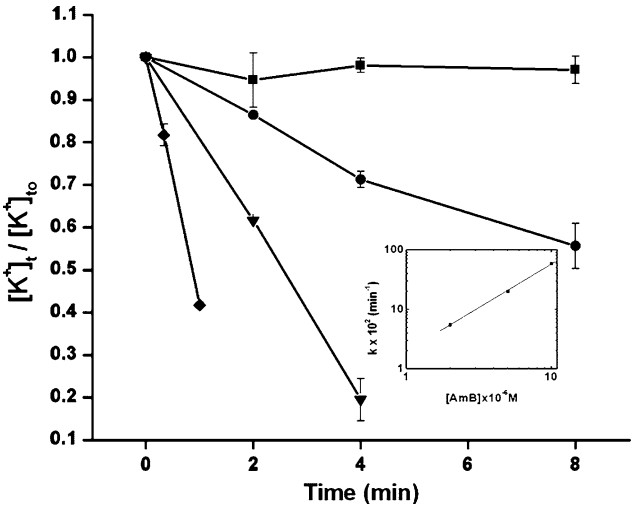

Fig. 1 Kinetics of K^+ efflux from erythrocytes treated with different concentrations of AmB. Log $[K^+]_t/[K^+]_o$ plotted versus time (in min). $[K^+]_t$ is the cell potassium concentration at time t; $[K^+]_o$ is the initial cell potassium concentration. *Filled square*, control; *filled circle*, 2 x 10^{-6} M AmB; *filled triangle*, 5 x 10^{-6} M AmB; *filled diamond*, 10 x 10^{-6} M AmB. *Inset* Rate constants (k) for K^+ efflux as a function of AmB concentration ($\times 10^{-6}$ M). k values were calculated from the slopes for each of the curves shown. Cells were suspended (2×10^8/ml) in NaCl–sucrose isotonic medium (pH 7.4). Data taken from an experiment carried out at 20°C (bars are SD for three to five experimental points)

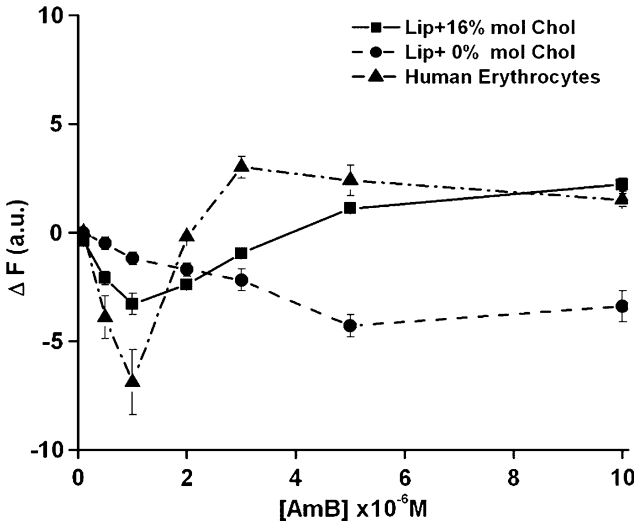

Fig. 2 Concentration dependence of AmB-induced fluorescence changes of $DiC_3(5)$ across liposomes and human erythrocytes. Liposomes were prepared (see "Materials and Methods") in 100 mM K-gluconate solution and suspended in a fluorescence cuvette containing 2 ml of 200 mM sucrose solution. Human erythrocytes (25×10^6/ml) were transferred to a fluorescence cuvette containing 2 ml of iso-osmotic sucrose buffer solution (pH 7.4). Ordinate, ΔF (in arbitrary units); abscissa, AmB concentration ($\times 10^6$ M). Calibration of polarization changes performed by adding valinomycin (2 μM) gave fluorescence values (ΔF in arbitrary units) of $-3.8.8 \pm 0.3$ (eggPC liposomes), -3.55 ± 0.4 (liposomes + 16% cholesterol) and 3.7 ± 0.8 (human erythrocytes). *Filled square*, liposomes prepared with 16 mol% cholesterol; *filled circle*, liposomes prepared without cholesterol; *filled triangle*, human erythrocytes

antibiotic concentration. For the data shown in Fig. 1, n is 1.46 ($r^2 = 0.99$). A separate determination of k for K^+ efflux across human erythrocytes carried out at five different AmB concentrations yielded an n of 1.6 ($r^2 = 0.985$).

The values of n obtained in the present work fall in the range 1.5–2.5, previously reported for AmB enhancement of erythrocyte permeability (Deuticke and Zollner 1972; Deuticke et al. 1973) and the value of 1.3 obtained for the dose–response curve of the AmB-induced cation conductance across skeletal muscle fibers (Shvinka and Caffier 1994). On the basis of the present data, it can be concluded that both the monomeric and the dimeric forms of the antibiotic are active forms that contribute to the formation of AmB channels.

Bimodal Effect of AmB on the Membrane Potential Across Membranes Containing or not Cholesterol

The linearity observed for the dose–response curves of the AmB-induced K^+ efflux across erythrocytes does not preclude that the total AmB action on the intracellular K^+ concentration can be due to the formation of more than one type of ion channel. Figure 2 shows the effect of AmB on the membrane potential across three different types of membranes, as measured by the equilibrium fluorescence changes (ΔF) of the membrane probe DiSC3(5) (see "Materials and Methods").

It can been in Fig. 2 (filled squares) that when liposomes prepared with 16 mol% cholesterol and loaded with potassium gluconate are suspended in an iso-osmotic sucrose solution, the addition of low AmB concentrations ($\leq 1 \times 10^{-6}$ M) produces (at equilibrium) a quenching of the probe fluorescence (ΔF), which reached a maximal value at 1.0×10^{-6} M AmB. Such an increased fluorescence quenching is very close to the negative polarization of the membrane potential that is measured in response to valinomycin, the highly selective K^+ ionophore (see legend to Fig. 2). It can also be observed in Fig. 2 that at concentrations higher than 1×10^{-6} M AmB produced a progressive decrease of the maximal quenching as the efflux of gluconate anions increases across the channels formed. At AmB concentrations higher than 4×10^{-6} M, a reversal to a positive enhancement of fluorescence is observed (Fig. 2). These results support the previous conclusion that the abrupt change in the salt or nonelectrolyte permeability induced across cholesterol-containing liposomes by AmB concentrations higher than 3×10^{-6} M (Cohen 1992) is due to the formation of aqueous pores permeable to monovalent cations and anions (Cohen 1992, 1998).

In liposomes prepared without sterols (Fig. 2, filled circles), the results of the ΔF measurements indicate that AmB produces a smaller but progressive quenching of the probe fluorescence, albeit at higher antibiotic concentrations. In fact, it can be observed in Fig. 2 that in the absence of sterols, ΔF attained its maximum value at 4×10^{-6} M AmB. It can also be seen that, under these conditions, the reversal of the negative enhancement of fluorescence across liposomes only becomes apparent after adding AmB at a concentration as high as 10×10^{-6} M (Fig. 2, filled circles).

The results of the ΔF measurements when AmB is added into human erythrocytes suspended in an iso-osmotic sucrose solution are also shown in Fig. 2 (filled triangles). It can be observed that low AmB concentrations ($\leq 1 \times 10^{-6}$ M) produce a progressive quenching of the probe fluorescence, indicating enhancement of the negative membrane potential by the AmB-induced K^+ efflux across erythrocyte membranes. As in the case of cholesterol-containing liposomes, the maximal quenching of the probe fluorescence has a value that is near that measured in response to valinomycin (see legend to Fig. 2). In erythrocyte membranes, AmB concentrations higher than 1×10^{-6} M also led to a reduction of the quenching, possibly due to chloride movement out of the cells across the channels formed, leading at 3×10^{-6} M AmB to an overall positive enhancement of fluorescence (Fig. 2, filled triangles).

It can thus be concluded from the data of Fig. 2 that the ion channels that are formed in cholesterol-containing liposomes and erythrocyte membranes by low concentrations of AmB ($\leq 1 \times 10^{-6}$ M) have a very high cation/anion selectivity ratio, whereas such selectivity abruptly decreases above a critical "threshold" AmB concentration, at which the aqueous pores are formed. The critical role that is played by cholesterol in the formation of aqueous pores is indicated by the observation that in liposomes prepared without sterols there is only a slight reversal of the negative enhancement of fluorescence and at AmB concentrations 10 times greater (Fig. 2, filled circles). Of note, the results in Fig. 2 also indicate that the formation of cation-selective nonaqueous channels in cholesterol-containing membranes by low AmB concentrations is facilitated by the presence of cholesterol, an effect that has been previously ascribed to the ability of sterols such as ergosterol or cholesterol to differentially modulate the acyl chain order of the membrane phospholipids (Cohen 1992; Venegas et al. 2003).

In agreement with the data shown in Fig. 2, Venegas et al. (2003) reported that in cholesterol-containing lipid bilayers AmB forms ion channels exhibiting not only the higher conductivities but also a reduced cation/anion selectivity. These authors also reported that AmB channels with high conductivities (so-called channel types V and VI) are observed in lipid bilayers prepared without sterols but only after adding very high concentrations of the polyene antibiotic (Venegas et al. 2003). It is not yet clear if the ion selectivity of the channels formed by high AmB concentrations in sterol-free lipid bilayers or in liposomes is different from that exhibited by the structures formed in cholesterol-containing membranes.

Finally, the ΔF equilibrium measurements in Fig. 2 show the strong similarity of the "threshold" concentration at which AmB produced a decrease of the membrane cation/anion selectivity in human erythrocytes compared to cholesterol-containing liposomes. However, as can be seen in Fig. 2, the AmB concentration range at which the two types of AmB channels responsible for this selectivity coexist in the membrane is much narrower in erythrocytes than in cholesterol-containing liposomes. Such a difference suggests that in erythrocyte membranes the interaction of AmB with cholesterol for the formation of the aqueous pores may be facilitated by the presence of membrane components that are absent in liposomes.

Effect of AmB on the Intracellular Concentrations of Na^+ and K^+ in Human Erythrocytes

When human erythrocytes are suspended in an iso-osmotic sodium-containing solution and treated with increasing AmB concentrations, the intracellular sodium and potassium concentrations ($[Na^+]_i$ and $[K^+]_i$) should be expected to increase and decrease, respectively, as a result of the Na/K exchange that is known to occur across the cation-selective AmB channels formed (Cybulska et al. 1995). Figure 3 shows the results of measurements of $[Na^+]_i$ and $[K^+]_i$ (at equilibrium) after AmB is added to human erythrocytes suspended in NaCl–sucrose (2:1) isotonic solution. The values plotted in Fig. 3 indicate that the $[Na^+]_i$ increase at low AmB concentrations reached a maximal value at about 3.0×10^{-6} M. In effect, $[Na^+]_i$ rose from 10.9 mM (control) to a maximum of 148 mM at 3.0×10^{-6} M. The corresponding $[K^+]_i$ decreased from an initial value of 93.4 to 4 mM at 3.0×10^{-6} M (Fig. 3). It can also be observed in Fig. 3 that at concentrations higher than 3.0×10^{-6} M, $[Na^+]_i$ abruptly decreased, reaching a value of 10 mM or lower.

Using the value for the external sodium concentration ($[Na^+]_e = 116$ mM, see "Materials and Methods") and the data shown in Fig. 3 for erythrocyte membranes treated with 3.0×10^{-6} M AmB, we can calculate the formation of a Nernst equilibrium potential of about −6 mV across the erythrocyte membranes (at room temperature). This calculated membrane potential is very close to the value of −9 mV that is known to be held across human erythrocytes under standard conditions (Hladky and Rink 1976). It can

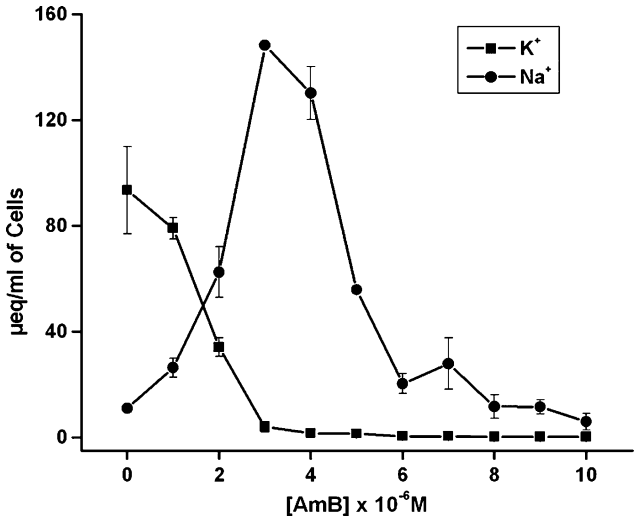

Fig. 3 Intracellular K^+ and Na^+ concentrations after incubation of cells with increasing AmB concentrations. Erythrocytes were suspended (2×10^8/ml) in NaCl–sucrose isotonic medium (pH 7.4) and incubated for 30 min at 37°C with different AmB concentrations. They were then centrifuged and washed two times with an isotonic solution of sucrose (pH 7.4) before being lysed as described in "Materials and Methods." Ordinate, µeq Na^+/ml cells (*filled circle*) and µeq K^+/ml cells (*filled square*); abscissa, AmB concentration ($\times 10^{-6}$ M)

then be concluded that the K^+/Na^+ exchange across the channels formed by AmB at low concentrations ($\leq 3.0 \times 10^{-6}$ M) is electroneutral since there are no appreciable AmB-induced changes in the normal cell membrane potential.

Since AmB has been reported to inhibit the Na–K pump across human erythrocytes at concentrations higher than 1.0×10^{-6} M (Vertut-Doi et al. 1988), a question arises about the possible influence of such inhibition on the results shown in Fig. 3. In this respect, the AmB-induced sodium influx can be calculated from the data of Fig. 3, by taking into account that the equilibrium $[Na^+]_i$ measurements were performed 30 min after adding the antibiotic (see "Materials and Methods"). The calculated sodium influx values are 30.8 and 274.8 mmol/l cell × h for 1.0 and 3.0×10^{-6} M AmB, respectively. These values are significantly greater than the mean value determined for the Na efflux through the ouabain-sensitive Na–K pump, 5.04 ± 0.72 mmol/l cells × h (Labonia et al. 1987), indicating clearly that the measured AmB-induced increases of $[Na^+]_i$ are not greatly affected by the presence of an active sodium pump protein taking ions out of the human erythrocytes.

Temperature Dependence of the AmB-Induced K^+ Efflux Across Human Erythrocytes

In order to further support the conclusion that the bimodal effects of increasing AmB concentrations on the membrane potential across cholesterol-containing membranes (Fig. 2) and ergosterol-containing leishmania membranes (Ramos et al. 1996; Cohen 1998) are due to the formation of two different types of channels by AmB, differing in their interactions with membrane sterol, we performed measurements of the temperature dependence of the K^+ efflux across human erythrocytes under different AmB concentrations (Fig. 4).

Figure 4 shows an Arrhenius plot (log k vs. 1/T) of the rate constants (k) determined for the K^+ efflux across human erythrocytes induced by 2.0, 5.0 and 10.0×10^{-6} M AmB at different temperatures. The temperature range (5–37°C) chosen was based on the physiological temperature of 37°C and the interest to measure the changes well below the structural changes that are known to occur in red cell membranes at about 20°C (Tanaka and Ohnishi 1976; Galla and Luisfetti 1980).

It can be observed in Fig. 4 that below 20°C (equivalent to $1/T = 3.413 \times 10^{-3}$ absolute degrees^{-1}), no significant changes of k with temperature were measured, independently of the AmB concentration added. In fact, in very close agreement with the results shown in Fig. 4, Wietzerbin et al. (1990) found that the corresponding Arrhenius plot for the K^+ efflux induced by addition of *N*-fructosyl-AmB across human erythrocytes (as measured by an independent ^{14}C-isotope-based technique) shows a break of

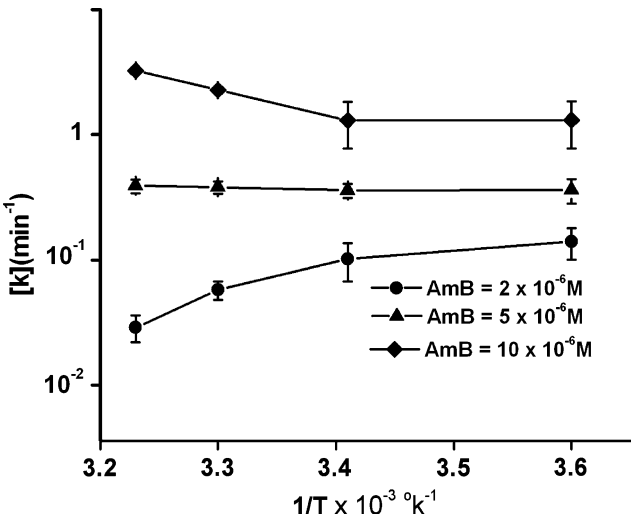

Fig. 4 Effect of temperature on the rate constant k for K^+ release from erythrocytes treated with AmB. Cells were suspended (2×10^8/ml) in NaCl–sucrose isotonic medium (pH 7.4) and AmB was added at different concentrations. Arrhenius plots of log k versus 1/T (°K) show potassium release data from cells treated with 2.0, 5.0 and 10.0×10^{-6} M AmB and incubated at 5, 20, 30 and 37°C. In all cases, AmB was dissolved in DMF. Control values (+1% DMF) for the rate constants were in all cases between 10^{-3} and 10^{-4} min^{-1}. Points are average values for three to eight separate experiments (±SD). Experimental points are connected with straight-line segments. *Filled circle*, 2 x 10^{-6} M AmB; *filled triangle*, 5 x 10^{-6} M AmB; *filled diamond*, 10 x 10^{-6} M AmB

the slope between 20 and 30°C, indicating that the antibiotic-induced permeability changes are sensitive to changes in the erythrocyte membrane fluidity resulting from the phase transition occurring at this temperature range (Tanaka and Ohnishi 1976; Galla and Luisfetti 1980).

Above the thermotropic temperature transition of the erythrocyte membrane, the curves corresponding to 2.0×10^{-6} and 10.0×10^{-6} M show a break of the slope but in opposite directions. Thus, whereas at the low concentration of 2.0×10^{-6} M AmB the rate constants decreased with rising temperature, at 10.0×10^{-6} M AmB the rate constants increased. Figure 4 also indicates that, at the intermediary AmB concentration of 5.0×10^{-6} M, the antibiotic-induced rate constants for the K^+ efflux were not significantly affected by temperature changes, clearly suggesting that two opposite processes, differently influenced by temperature, are affecting the channel formation by AmB. Table 1 lists the calculated activation energy (E_a) values for the corresponding K^+ efflux induced by different AmB concentrations.

Temperature Dependence of the AmB-Induced Ca^{2+} Influx Across Human Erythrocytes

The aqueous pores that are formed by AmB across ergosterol- and cholesterol-containing liposomes are permeable to nonelectrolytes as large as glucose (Cohen 1992), large anions such as gluconate (Fig. 2) and divalent Ca^{2+} ions (Ramos et al. 1989). In human monocytes, it has also been shown (Rogers et al. 1999) that AmB is able to increase the intracellular calcium concentration with a maximal effect between 2×10^{-6} and 5×10^{-6} M.

We measured the effect of increasing AmB concentrations on the calcium influx across human erythrocytes (see "Materials and Methods") at two different temperatures 5 and 37°C (Table 2). It can be seen in Table 2 that addition of AmB to ATP-free human erythrocytes (see "Materials and Methods") leads to a significant enhancement of Ca^{2+} influx but only after adding AmB concentrations higher than 2×10^{-6} M. It can also be seen in Table 2 that the k values determined for both AmB concentrations increase at higher temperatures, leading to positive values of E_a for the formation of the aqueous pores.

Table 1 E_a values for AmB-induced K^+ permeability across human erythrocyte membranes

[AmB] ($\times 10^{-6}$ M)	E_a (kcal/mol)
2	-13.8 ± 1.6
5	0.9 ± 0.1
10	10.8 ± 2.1

E_a values were calculated using the k values from K^+ release from cells measured between 20 and 37°C (see Fig. 3). Average ± SD for three independent experiments

Table 2 Effect of increasing AmB concentrations and temperatures on net Ca^{2+} influx across human erythrocyte membranes

[AmB] ($\times 10^{-6}$ M)	$[Ca^{2+}]_f - [Ca^{2+}]_i$ (μmoles total Ca^{2+}/ml cells)	
	5°C	37°C
0[a]	$+0.07 \pm 0.01$	-0.08 ± 0.01
2	-0.14 ± 0.05	-0.20 ± 0.04
5	0.02 ± 0.05	0.22 ± 0.1
10	0.62 ± 0.1	0.99 ± 0.3

Erythrocytes were preincubated at 37°C and 25% hematocrit for 1 h in the dark with iodoacetate (1 mM) to inhibit the Ca^{2+} pump (see "Materials and Methods"). For measurements of calcium influx, cells (10% hematorit or 8×10^8 cells) were suspended for 30 min in medium containing (mM) KCl 110, sucrose 62, calcium chloride 10 mM, Tris–HCl (at pH 7.4) and different AmB concentrations. The AmB stock solution (1 mM) was prepared in DMSO. The calcium concentration in erythrocytes before preincubation was 20 nmoles/ml cells. Net calcium influx: $[Ca^{2+}]_f - [Ca^{2+}]_i$, f, final; i, initial)

[a] Control + 5% DMSO, average ± SD (three experiments)

Effect of TT on the AmB-Induced K^+ Efflux Across Human Erythrocytes

The near zero values that we measured for the E_a of the K^+ efflux induced by intermediate concentrations of AmB across erythrocyte membranes (Fig. 4) can then be taken as an indication that the two different types of channels formed by AmB in erythrocyte membranes coexist simultaneously, leading at 5×10^{-6} M to a near cancellation of the opposite values that are generated by the E_a of each of them (Table 1). Due to the heterogeneity of the erythrocyte membranes, it is also likely that the two types of channels may be formed in different membrane regions, differing in lipid composition and/or cholesterol content. This possibility was investigated using TT, an oxidative agent that by cross-linking the cytoskeleton protein spectrin is known to produce a partial loss of the membrane asymmetry of the phospholipids (Haest et al. 1978).

The data in Table 3 show that the k values for K^+ efflux measured for the control erythrocytes (not incubated with TT) and treated with 2×10^{-6} M AmB decreased when the temperature was raised from 5 to 37°C. By contrast, when control erythrocytes were treated with 10×10^{-6} M AmB, the corresponding k values for K^+ efflux increased over the same temperature range (top values in Table 3). The calculated Q ratios ($k_{37°C}/k_{5°C}$) shown in Table 3 are in agreement with the measured negative and positive values of E_a, respectively, for the K^+ permeabilization induced by low and high AmB concentrations (Table 1).

Table 3 Effect of TT on AmB-induced rate constants (k) for K^+ efflux across human erythrocyte membranes at different temperatures

[TT] (mM)	T (°C)	Control k (min^{-1})	2×10^{-6} M AmB/ k (min^{-1})	$Q_{37/5}$	10×10^{-6} M AmB/ k (min^{-1})	$Q_{37/5}$
Control	5	$0.002 \pm 5 \times 10^{-4}$	0.25 ± 0.02	0.2	1.97 ± 0.2	1.6
	37	0.003 ± 0.001	0.05 ± 0.1		3.1 ± 0.3	
2	5	0.003 ± 0.001	0.23 ± 0.03	0.4	2.1 ± 0.3	1.3
	37	0.008 ± 0.002	0.1 ± 0.05		2.8 ± 0.5	
20	5	0.002 ± 0.001	0.37 ± 0.1	0.7	3.0 ± 0.4	1.1
	37	0.008 ± 0.002	0.26 ± 0.05		3.1 ± 0.5	

$Q_{37/5} = k_{37°C}/k_{5°C}$. Average ± SD (triplicate experiments). k values for K^+ permeability in control cells, incubated or not with TT, are very small compared with values obtained after adding AmB

Upon incubation with two different TT concentrations (2 and 20 mM TT, see "Materials and Methods"), erythrocytes treated with 2×10^{-6} M AmB exhibited an increase of the K^+ k at low and high temperatures. However, it can be seen that such an increase of the AmB-induced K^+ permeability was significantly higher at 37°C than at 5°C, leading to a $Q_{k37/k5}$ ratio that increased from 0.2 (in control cells) to 0.4 (in cells incubated with 2 mM TT) and 0.7 (in cells incubated with 20 mM TT). By contrast, when cells were incubated with TT but treated with 10×10^{-6} M AmB, the $Q_{k37/k5}$ ratios decreased from 1.6 (in control cells) to 1.3 (in cells incubated with 2 mM TT) and 1.1 (in cells incubated with 20 mM TT) (Table 3).

Discussion

On the basis of our previous work with liposomes and sterol-containing sensitive organisms such as *Leishmania* sp., we have proposed that AmB action on biological membranes is mediated by the formation of two types of ionic channels, nonaqueous channels and aqueous pores, differing in permeability properties (Cohen 1992, 1998; Ramos et al. 1996). Thus, the nonaqueous channels formed by AmB at low concentrations are permeable to monovalent cations (such as K^+ and Na^+) but impermeable to anions and divalent cations. By contrast, the aqueous pores formed by AmB at higher concentrations are permeable to monovalent anions as well as to monovalent and divalent cations such as Ca^{2+}. In this two-stage mechanism of AmB action, (1) low concentrations of AmB cause K^+ leakage from sensitive cells, but the lethal or more toxic effects are only produced after a certain "critical" concentration, which is required for the formation of aqueous pores, is reached at the membrane phase; and (2) the formation of aqueous pores is dependent on the interaction of AmB with either membrane ergosterol or cholesterol molecules.

The permeabilizing effects that we have measured in the present work for the action of AmB on liposomes and erythrocyte membranes support these conclusions, indicating that the polyene antibiotic can form two types of membrane ion channels in cholesterol-containing human erythrocytes, depending on the AmB concentration (Fig. 2). Of significance, the present measurements of the E_a of channel formation (Fig. 4, Tables 1 and 2) allow us to distinguish the two distinct types of ion channels that are formed by AmB in erythrocyte membranes. In this respect, although several authors have reported E_a measurements for the AmB-induced ion permeabilities in different types of membranes that are both negative and positive (De Kruijff et al. 1974; Archer 1976; Bolard et al. 1991; Cohen 1992; Shvinka and Caffier 1994; Venegas et al. 2003), no explanation for such opposite effects has been proposed.

In order to understand the origin of such opposite effects of temperature on the magnitude of the AmB-induced permeabilizing action, it is necessary to take into account that the rate of ion flux induced by AmB across membranes is a function of the number of channels formed per cell and the ionic permeability of the channels once formed. The first factor depends on the interactions of AmB molecules with the lipid components of the membrane, whereas the second factor depends on the intrinsic permeability properties of the channels and their stability. However, since ionic diffusion thorough the AmB channels themselves is very fast (Cybulska et al. 1986), this last step does not limit the overall rate process. It follows that, in a first approximation, the energy of formation of the channels at the membrane is the main energetic barrier for the measured AmB-induced permeability changes. Such a process can be separated into the following events: the adsorption of polyene antibiotic molecules into the membrane surface, the insertion of small oligomers between the phospholipid chains to form nonaqueous AmB channels and the interaction of membrane-bound AmB monomers, or inserted prepore AmB channels, with sterol molecules to form aqueous pores.

Concerning the adsorption step, studies of the binding kinetics of several AmB derivatives into human erythrocytes have indicated that such a step is almost instantaneous, provided that in the aqueous solution the monomeric

form of the antibiotic predominates (Wietzerbin et al. 1990). Wietzerbin et al. (1990) also found that the binding rate of *N*-fructosyl AmB increased with raising temperatures and, as a result, small positive activation energies were calculated. According to these authors, the small positive activation energy for the binding kinetics of AmB derivatives into erythrocyte membranes may reflect the breaking of H-bonds formed between the hydroxyl groups of the AmB derivative molecule and the polar heads of the phospholipids at the membrane–water interface.

The second step in the sequence of events leading to channel formation by the AmB molecules corresponds to the simultaneous insertion/penetration of several AmB monomers into the membrane to form nonaqueous channels, a process that is thermodynamically favored by the hydrophobic interactions of the polyene side of the macrolide ring with the hydrocarbon chains of the phospholipids. The predominance of the hydrophobic forces in the formation of the nystatin ion channels in lipid bilayers was first reported by Cass et al. (1970), who demonstrated that the equilibrium conductance induced by nystatin abruptly decreased with the rise of temperature as a consequence of the increased destruction rate of the ionic channels formed. In the present work, the measured activation energy for K^+ efflux induced by a low AmB concentration in erythrocyte membranes yielded also a negative value of −13.8 Kcal/mole (Table 1), indicating that hydrophobic forces between lipids and AmB molecules predominate in the multimolecular assembling of such channels.

Other authors have proposed that the origin of the negative values for the temperature dependence of the AmB-induced ion permeability changes can be explained by the decrease of the amount of self-associated forms with temperature because this parameter is also known to be driven by hydrophobic forces (Lambing et al. 1993). However, the contribution of temperature changes to the relative amounts at the aqueous medium of the monomeric versus self-associated AmB molecules is expected to be extremely small because very few channels actually need to be formed across a membrane to be able to dissipate completely the transmembrane ionic gradient. This prediction is also supported by the partition data obtained for nystatin in liposome membranes, which have indicated that the polyene molecules occupy <1% of the external surface area of liposomes at a concentration which is fully capable of dissipating the ionic gradient across such vesicles (Coutinho et al. 2004).

Following the formation of the predominantly cation-selective nonaqueous channels by AmB, the aqueous pores are proposed to be formed by the interaction of the nonaqueous AmB channels with cholesterol molecules. The measured positive values for the activation energy of the K^+ efflux (Table 1) and calcium influx (Table 2) above the "threshold" AmB concentration can be rationalized on the basis that the association rate constant for the formation of complexes between AmB and cholesterol molecules increases with temperature. In fact, the formation in water of amphotericin B/cholesterol complexes is known to yield positive energies of activation (Ernst et al. 1979). In this respect, since the formation of such complexes in the membrane involves the subtraction of cholesterol molecules from their interactions with other lipid membrane components, such a process is also expected to yield positive energies of activation due to the breaking of the H-bonds, which are known to be established between the sterol and lipid polar head groups (Barenholz 2002).

The rapid dissipation of the transmembrane sodium gradient across erythrocyte membranes that we have measured at AmB concentrations higher than 3×10^{-6} M (Fig. 3) may be ascribed to an increased stability of the ion channels formed by AmB at such concentrations. Thus, it is likely that the AmB molecules forming the aqueous pores, due to complexation with membrane cholesterol, can no longer exchange rapidly with the aqueous phase during the washing phase of the cells that is performed before the ion measurements are made (see legend to Fig. 3). Of note, this behavior was not observed in skeletal muscle fibers (Shvinka and Caffier 1994) as the conductance changes induced by AmB were found to be completely reversible after washing the fibers in antibiotic-free solutions. Importantly, the measurements of the effect of temperature on the conductance changes induced by AmB across such fibers yielded negative energies of activation at concentrations as high as 10.0×10^{-6} M AmB (Shvinka and Caffier 1994), an indication that in these skeletal muscle membranes the exchange with the aqueous phase of the AmB molecules forming the ion channels occurs readily, driven by hydrophobic forces up to relatively high AmB concentrations. The observed difference in the reversibility of AmB-induced permeability changes in different cell types is an indication that the formation of AmB/cholesterol complexes may depend on specific membrane factors, i.e., relative enrichment of saturated hydrocarbon chains, that may facilitate the insertion of AmB molecules in cholesterol-containing lipid rafts.

Effect of TT

Our interpretation of the results obtained for the effect of temperature on the AmB-induced K^+ permeabilities across erythrocytes incubated with TT (Table 3) is based on the assumption discussed above that the formation of cholesterol-dependent channels yields positive activation energies, whereas the formation of cholesterol-independent channels yields negative activation energies of formation. Of significance, the observed decrease of the Q ratios

($k_{37°C}/k_{5°C}$) from 1.6 (control) to 1.1 in TT-treated erythrocytes exposed to 10.0×10^{-6} M AmB (Table 3) indicates that the formation of aqueous pores substantially decreases at polyene concentrations at which the cholesterol-dependent structures predominate in the membranes (Fig. 2). This effect may originate from the disruption by TT of the interactions between spectrin and the sterol-rich lipid rafts (Salzer and Prohaska 2001; Ciana et al. 2005; Crepaldi Domingues et al. 2009). Such a disruption of the spectrin–lipid raft interactions may be an important factor that leads to the TT-induced loss of the membrane phospholipid asymmetry of the erythrocyte membrane (Haest et al. 1978), including a decrease in the amount of sphingomyelin (a lipid rich in saturated hydrocarbon chains) that is normally enriched at the outer leaflet. As a consequence, the insertion of AmB molecules in the membrane lipid rafts as well as the subsequent formation of aqueous pores within such microdomains would decrease as these processes are known to be facilitated by ordered saturated membrane domains (Cohen 1992; Czub and Baginski 2006).

On the other hand, the observed increase of the Q ratios ($k_{37°C}/k_{5°C}$) from 0.2 to 0.7 for TT-treated erythrocytes exposed to 2.0×10^{-6} M AmB (Table 3) is an indication that the activation energies for channel formation are less negative. This effect may originate from an increased formation of cholesterol-dependent aqueous pores in non-lipid raft regions due to enhanced exposure of the membrane cholesterol at the outer leaflet. In fact, as recently demonstrated by Lange et al. (2007), loss of the membrane asymmetry of the phospholipids in erythrocyte membranes always leads to increased exposure of the cholesterol at the outer leaflet. The reason for this effect is that the externalization of phosphatidylserine (PS) will determine that phosphatidylcholine and sphingomyelin, the phospholipids which are more strongly associated with cholesterol, are no longer predominant at the outer leaflet. In this respect, it is important to note that Szponarski and Bolard (1987) have previously demonstrated the formation of AmB/cholesterol complexes in human erythrocytes but only after cell ghosts were incubated into a low ionic strength buffer, a treatment that is now known to lead to an increase of outer membrane cholesterol as a consequence of PS externalization (Lange et al. 2007).

Origin of the Ion Selectivity of AmB Channels

In order to account for the observed AmB-induced permeability to larger molecules such as glucose (Cohen 1992) and cations such as calcium (Table 2), we have proposed that the aqueous pores formed by AmB beyond a certain "threshold" concentration have an increased pore radius compared to the predominantly cation-selective nonaqueous channels formed at low AmB concentrations (Cohen 1998). In this regard, implicit in describing the second type of structures formed as "aqueous pores" is the consideration of the state of water within the channel. Such an operational definition has been based on the observation that the formation of AmB aqueous pores is always accompanied by a decrease of the reflection coefficient of urea (Cohen 1992, 1998), a behavior that indicates that urea permeates by passage through an aqueous channel, as originally observed in planar lipid bilayers (Finkelstein and Holz 1973). In fact, the irreversible thermodynamic parameter, σ_i, the reflection coefficient, is a measure of the relationship between the permeability of the solute and that of water. Recently, molecular dynamics simulations of water behavior in nanopores have revealed that water can fill the ion channels but only when such channels reach a critical radius (R_C), whose magnitude depends on the chemical characteristics of the pore walls (Allen et al. 2002; Beckstein and Sansom 2004). The calculated R_C is about 0.29 nm for a pore with an amphipathic wall, a value that is significantly smaller than the pore radius of 0.43 nm that was obtained for the AmB aqueous pores by applying a continuum fluid hydrodynamic theory to pores of molecular dimensions (Finkelstein and Holz 1973). Interestingly, a grand canonical Monte Carlo simulation of a simplified ion channel model with a pore radius of 0.35 nm has indicated (Boda et al. 2007) that the Ca/Na selectivity increases dramatically when the dielectric coefficient e within the channel increased from 10 to 80 (bulk water), a result that may simulate the behavior observed when the ion channels formed by AmB at low concentrations slightly increase radius to fill with water and form the aqueous pores.

In summary, we conclude from the present findings that AmB forms two types of channels in cholesterol-containing human erythrocytes, above and below a critical "threshold" concentration. It is demonstrated that such channels can be clearly distinguished by measuring their overall activation energies of formation. Analysis of the origin of the activation energies for the cation-selective ion channels indicated that they are formed without the direct participation of sterol molecules, as indicated by the predominance of hydrophobic forces that enhanced their formation at lower temperatures. By contrast, the formation of AmB aqueous pores is associated with positive energies of activation, possibly due to the interaction of AmB molecules with sterol via the disruption of the H-bond interactions between cholesterol and other lipid membrane components. In agreement with the therapeutic values commonly used for AmB treatment of systemic fungal infections, the present results also indicate that the concentration range above which the AmB aqueous pores are predominantly formed in human erythrocyte membranes (1×10^{-6} to

3×10^{-6} M) is very close to the plasma concentration range (1.5×10^{-6} to 2.1×10^{-6} M) which is tolerable in patients treated with 1 mg/kg of AmB mixed with deoxycholate (Heinemann et al. 1997). As we previously suggested (Cohen 1998), the increased safety profile and decreased nephrotoxicity exhibited by the various lipid formulations of AmB compared to the conventional deoxycholate AmB can be explained by the ability of the lipid formulations to prevent formation of the more toxic aqueous pores in the membranes of host cells, while retaining such a capacity in the membranes of sensitive pathogens.

Acknowledgement The authors are indebted to Prof. Pedro J. Romero for providing access to the facilities and equipment of his laboratory at the Central University of Venezuela to perform the experiments with human erythrocytes.

References

Allen R, Melchionna S, Hansen J-P (2002) Intermittent permeation of cylindrical nanopores by water. Phys Rev Lett 89:175502–175504

Archer DB (1976) Effect of the lipid composition of *Mycoplasma mycoides* subspecies capri and phosphatidyl choline vesicles upon the action of polyene antibiotics. Biochim Biophys Acta 436:68–76

Barenholz Y (2002) Cholesterol and other membrane active sterols: from membrane evolution to "rafts". Prog Lipid Res 41:1–5

Beckstein O, Sansom MSP (2004) The influence of geometry, surface character and flexibility on the permeation of ions and water though biological pores. Phys Biol 1:42–52

Boda D, Valisko M, Eisenberg B, Nonner W, Henderson D, Gillespie D (2007) Combined effects of pore radius and protein dielectric coefficient on the selectivity of a calcium channel. Phys Rev Lett 98:168102–168104

Bolard J, Legrand P, Heitz F, Cybulska B (1991) One-sided action of amphotericin B on cholesterol-containing membranes is determined by its self-association in the medium. Biochemistry 30:5707–5715

Cass A, Finkelstein A, Krespi V (1970) The ion permeability induced in thin lipid membranes by the polyene antibiotics nystatin and amphotericin B. J Gen Physiol 56:100–124

Ciana A, Balduini C, Minetti G (2005) Detergent-resistance membranes in human erythrocytes and their connection to the membrane skeleton. J Biosci 30:317–328

Cohen BE (1975) The permeability of liposomes to non-electrolytes. II. The effect of nystatin and gramicidin A. J Membr Biol 20:235–260

Cohen BE (1992) A sequential mechanism for the formation of aqueous channels by amphotericin B in liposomes. The effect of sterols and phospholipid composition. Biochim Biophys Acta 1108:49–58

Cohen BE (1998) Amphotericin B toxicity and lethality: a tale of two channels. Int J Pharmaceutics 162:95–106

Coutinho A, Silva L, Fedorov A, Prieto M (2004) Cholesterol and ergosterol influence nystatin surface aggregation: relation to pore formation. Biophys J 87:3264–3276

Crepaldi Domingues C, Ciana A, Buttafava A, Balduini C, De Paula E, Minetti G (2009) Resistance of human erythrocyte membranes to triton X-100 and $C_{12}E_6$. J Membr Biol 227:39–48

Cybulska B, Herve M, Borowski E, Gary-Bobo CM (1986) Effect of the polar head structure of polyene macrolide antifungal antibiotics on the mode of permeabilization of ergosterol- and cholesterol-containing lipidic vesicles studied by ^{31}P-NMR. Mol Pharmacol 29:293–298

Cybulska B, Bolard J, Seksek O, Czerwinski A, Borowski E (1995) Identification of the structural elements of amphotericin B and other macrolide antibiotics of the heptaene group influencing the ionic selectivity of the permeability pathways formed in the red cell membrane. Biochim Biophys Acta 1240:167–178

Czub J, Baginski M (2006) Comparative molecular dynamics study of lipid membranes containing cholesterol and ergosterol. Biophys J 90:2368–2382

De Kruijff B, Demel RA (1974) Polyene antibiotic–sterol interactions in membranes of *Acholesplasma laidlawii* cells and lecithin liposomes. III. Molecular structure of the polyene antibiotic-cholesterol complexes. Biochim Biophys Acta 339:57–70

De Kruijff B, Gerritsen WJ, Oerlemanns A, Van Dick PW, Demel RA, Van Deenen LLM (1974) Polyene antibiotic–sterol interactions in membranes of *Acholeplasma laidlawii* cell and lecithin liposomes. II. Temperature dependence of the polyene antibiotic–sterol complex formation. Biochim Biophys Acta 339:44–56

Deuticke B, Zollner C (1972) Lack of influence of membrane cholesterol on anion and nonelectrolyte permeability of pig erythrocytes. Biochim Biophys Acta 266:726–731

Deuticke B, Kim M, Zollner C (1973) The influence of amphotericin B on the permeability of mammalian erythrocytes to nonelectrolytes, anions and cations. Biochim Biophys Acta 318:345–359

Dodge JT, Mitchell C, Hanahan DJ (1963) The preparation and chemical characteristics of hemoglobin-free ghosts of human erythrocytes. Arch Biochim Biophys 100:119–130

Drabkin DL, Austin JH (1932) Spectroscopy studies. I. Spectrophotometric constants for common hemoglobin derivatives in human, dog and rabbit blood. J Biol Chem 98:719–733

Ernst C, Lematre J, Tinnert H, Dupont G, Grange J (1979) Interaction between an antifungal heptaene, amphotericin B and cholesterol in vitro, as detected by circular dichroism and absorption. Influence of temperature. C R Seances Acad Sci D 289:1145–1149

Finkelstein A, Holz R (1973) Aqueous pores created in thin lipid membranes by the polyene antibiotic nystatin and amphotericin B. In: Eisenman G (ed) Membranes, vol 2. Marcel Deckker, New York, pp 377–408

Galla H-J, Luisfetti J (1980) Lateral and transversal diffusion and phase transitions in erythrocyte membranes. An excimer fluorescence study. Biochim Biophys Acta 596:106–117

Gallis HA, Drew RH, Pickard WW (1990) Amphotericin B: 30 years of clinical experience. Rev Infect Dis 12:308–329

Grzybeck M, Chorzlska A, Bok E, Hryniewicz A, Czogalla A, Diakowski W, Sikorski AF (2006) Spectrin–phospholipid interactions. Existence of multiple kinds of binding sites? Chem Phys Lipids 141:133–141

Haest CWM, Plasa G, Kamp D, Deuticke B (1978) Spectrin as a stabilizer of the phospholipid asymmetry in the human erythrocyte membrane. Biochim Biophys Acta 509:21–32

Heinemann V, Bosse D, Jehn U, Kahny B, Wachholz K, Debus A, Scholz P, Kolb H-J, Wilmanns W (1997) Pharmacokinetics of liposomal amphotericin B (AmBisome) in critically ill patients. Antimicrob Agents Chemother 41:1275–1280

Hladky SB, Rink TJ (1976) Potential difference and the distribution of ions across the human red blood cell membrane: a study of the mechanism by which the fluorescent cation, diS-C3-(5) reports membrane potential. J Physiol 263:287–319

Koumanov KS, Tessier C, Monchilova AB, Rainteau D, Wolf C, Quinn PJ (2005) Comparative lipid analysis and structure of

detergent-resistant membrane raft fractions isolated from human and ruminant erythrocytes. Arch Biochim Biophys 434:150–158

Labonia WD, Morelli OH Jr, Gimenez MI, Freuler PV, Morelli OH (1987) Effects of L-carnitine on sodium transport in erythrocytes from dialyzed uremic patients. Kidney Int 32:754–759

Laemmli WK (1970) Cleavage of structural proteins during the assembly of the head by bacteriophage T4. Nature 227:680–685

Lambing HE, Wolf WD, Hartsel SC (1993) Temperature effects on the aggregation state and activity of amphotericin B. Biochim Biophys Acta 1152:185–188

Lange Y, Ye J, Steck TL (2007) Scrambling of phospholipids activates red cell membrane cholesterol. Biochemistry 46:2233–2238

Legrand P, Romero EA, Cohen BE, Bolard J (1992) Effects of aggregation and solvent on the toxicity of amphotericin B to human erythrocytes. Antimicrob Agents Chemother 36:2518–2522

Nebl T, Pestonjamasp KN, Leszyk JD, Crowley JL, Oh SW, Luna EJ (2002) Proteomic analysis of a detergent-resistant membrane skeleton from neutrophil plasma membranes. J Biol Chem 277:43399–43409

Ohvo-Rekila H, Ramstedt B, Lppimaki P, Slotte JP (2002) Cholesterol interactions with phospholipids in membranes. Prog Lipid Res 41:66–97

Ramos H, Attias de Murciano A, Cohen BE, Bolard J (1989) The polyene antibiotic amphotericin B acts as a Ca^{2+} ionophore across sterol-containing liposomes. Biochim Biophys Acta 982:303–306

Ramos H, Valdivieso E, Gamargo M, Dagger F, Cohen BE (1996) Amphotericin B kills unicellular leishmanias by forming aqueous pores permeable to small cations and anions. J Membr Biol 152:65–75

Readio J, Bittman R (1972) Equilibrium binding of amphotericin B and its methyl ester and borate complex to sterols. Biochim Biophys Acta 685:219–224

Rogers PD, Kramer RE, Chapman SW, Cleary JD (1999) Amphotericin B-induced interleukin-1beta expression in human monocyte cells is calcium and calmodulin dependent. J Infect Dis 180:1259–1266

Romero PJ, Romero EA (1997) Differences in Ca^{2+} pumping activity between sub-populations of human red cells. Cell Calcium 21:353–358

Salzer U, Prohaska R (2001) Stomatin, flotillin-1, and flotillin-2 are major integral proteins of erythrocyte lipid rafts. Blood 97:1141–1143

Shvinka N, Caffier G (1994) Cation conductance and efflux induced by polyene antibiotics in the membrane of skeletal muscle fiber. Biophys J 67:143–152

Silva L, Coutinho A, Fedorova A, Prieto M (2006) Competitive binding of cholesterol and ergosterol to the polyene antibiotic nystatin. A fluorescent study. Biophys J 90:3625–3631

Simons K, Vaz WL (2004) Model systems, lipid rafts and cell membranes. Annu Rev Biophys Biomol Struc 33:269–295

Sundar S, Chakravarty J, Rai VK, Agrawal N, Singh SP, Chauhan V, Murray HW (2007) Amphotericin B treatment for Indian visceral leishmaniasis: response to 15 daily versus alternate-day infusions. Clin Infect Dis 45:556–561

Szponarski W, Bolard J (1987) Temperature-dependent modes for the binding of the polyene amphotericin B to human erythrocyte membranes: a circular dichroism study. Biochim Biophys Acta 897:229–237

Tanaka KI, Ohnishi S (1976) Heterogeneity in the fluidity of intact erythrocyte membrane and its homogenization upon hemolysis. Biochim Biophys Acta 426:218–231

Van Hoogevest P, DeKruijff B (1978) Effect of amphotericin B on cholesterol-containing liposomes of egg phosphatidylcholine and didocosenoyl phosphatidylcholine. A refinement of the model for the formation of pores by amphotericin B in membranes. Biochim Biophys Acta 511:397–407

Venegas V, Gonzalez-Damian J, Celis H, Ortega-Blake I (2003) Amphotericin B channels in the bacterial membrane: role of sterol and temperature. Biophys J 85:2323–2332

Vertut-Doi A, Hannaert P, Bolard J (1988) The polyene antibiotic amphotericin B inhibits the Na^+/K^+ pump of human erythrocytes. Biochem Biophys Res Commun 157:692–697

Wietzerbin J, Szponarski W, Gary-Bobo C (1990) Kinetic study of interaction between [^{14}C] amphotericin B derivatives and human erythrocytes; relationship between binding and induced K^+ leak. Biochim Biophys Acta 1026:93–98